REVIEW

Up-Conversion Luminescent Nanoparticles for Molecular Imaging, Cancer Diagnosis and Treatment

Shuihong Li[1],[*]
Xiaodan Wei[2],[*]
Sisi Li[1]
Cuiming Zhu[1]
Chunhui Wu[2]

[1]Institution of Pathogenic Biology, Hengyang Medical College, University of South China, Hengyang 421001, Hunan, People's Republic of China; [2]School of Life Science and Technology, University of Electronic Science and Technology of China, Chengdu 610054, Sichuan, People's Republic of China

*These authors contributed equally to this work

Abstract: In the past few years, we have witnessed great development and application potential of various up-conversion luminescent nanoparticles (UCNPs) in the nanomedicine field. Based on the unique luminescent mechanism of UCNPs and the distinguishable features of cancer biomarkers and the microenvironment, an increasing number of smart UCNPs nanoprobes have been designed and widely applied to molecular imaging, cancer diagnosis, and treatment. Considerable technological success has been achieved, but the main obstacles to oncology nanomedicine is becoming an incomplete understanding of nano–bio interactions, the challenges regarding chemistry manufacturing and controls required for clinical translation and so on. This review highlights the progress of the design principles, synthesis and surface functionalization preparation, underlying applications and challenges of UCNPs-based probes for cancer bioimaging, diagnosis and treatment that capitalize on our growing understanding of tumor biology and smart nano-devices for accelerating the commercialization of UCNPs.

Keywords: multimodal imaging, cancer biomarkers, tumor microenvironment

Correspondence: Shuihong Li
Institution of Pathogenic Biology, Hengyang Medical College, University of South China, Hengyang 421001, Hunan, People's Republic of China
Tel/Fax +86 734 8282907
Email zhoubaoxi520@163.com

Chunhui Wu
School of Life Science and Technology, University of Electronic Science and Technology of China, Chengdu 610054, Sichuan, People's Republic of China
Tel/Fax +86 28 83203353
Email wuchunhui@uestc.edu.cn

Introduction

Inorganic nanoparticles of rare-earth (RE) element lanthanide have attracted a great deal of attention. Their quality of high penetration into tissues, low damage to biological samples, flexibility for storage, sharp emission bands, and resistance to auto-fluorescence interference has been reported.[1,2] RE nanoparticles have become an ideal biomaterial choice for multi-modal tumor imaging, drug delivery, photo-dynamic therapy (PDT), and photo-thermal therapy (PTT) because of the up-conversion luminescence mechanism.[3,4] The up-conversion luminescence refers to a non-linear optical process involved in continuous multiphoton absorption and the interionic energy transfer, in which low-energy photons are converted into one high-energy (with short wavelength) emission.[5] The luminescent property of up-conversion nanoparticles (UCNPs) shows obvious advantage compared to down-conversion nanoparticles including organic fluorescent dyes and semiconductor quantum dots that were often used for bio-labelling. Conventional fluorescent probes cannot resolve the problem of photobleaching-induced intermittent detection, however, UCNPs exhibit longer fluorescence lifetime and higher fluorescence stability.[6,7] In recent years, UCNPs have gained increasing attention for various applications ranging from bioimaging to cancer therapy.[1,8]

Cancer is a life-threatening disease all over the world without an efficient cure. Cancer is the second leading cause of death in the United States and the third

leading cause of death in the People's Republic of China.[9] Surgery, chemotherapy and radiation therapy are the most commonly used treatments.[10] For early-stage solid tumor, surgery has been considered as the first choice for treatment.[11] Imaging technology has promoted the development of precision medicine in cancer diagnosis and therapy.[12] Oncologic surgery requires precise removal of tumor through accurate visualization without damage to normal tissues.[13] Ultrasound, magnetic resonance imaging (MRI) and computed tomography (CT) are three major imaging paths for cancer diagnosis, however, these imaging tools could not work well for early-stage small tumors. Three important elements: early detection, accurate lesion positioning and real-time intraoperative monitoring (RTIM) would be necessary for developing precise imaging used in cancer diagnosis and surgery. Since molecular imaging was first introduced in 1999 by Weissleder,[14] medical imaging has developed to a new era. Positron emission tomography (PET) and 18F-NaF imaging with the calcification process had been used in imaging of coronary arteries, which is a typical example of cardiovascular molecular imaging.[15] The molecular imaging is a combination of a well-designed molecular probe with an external detection system.[16] As a new generation of imaging technology, molecular imaging will develop novel insights into cancer as well as novel diagnosis and therapy.[17] Unlike conventional imaging, molecular imaging works at the molecular level by analyzing the membrane proteins, secreted proteases, receptors, and other molecular biomarkers of tumor cells.[18,19]

UCNPs display a more superior performance than other candidates due to the good stability, high sensitivity, low toxicity, deep penetration, excellent biocompatibility and low interference with background fluorescence.[20] Therefore, UCNPs have become a research highlight for developing bioimaging. A growing number of molecular-imaging probes, especially rare-earth up-conversion fluorescent probes, have been successfully used to target tumors and distinguish tumor from non-tumor tissues, which further contributed to reveal the location and region of tumor cells.[13,21] Here, we mainly reveal the potential usages of UCNP-based fluorescent probes for tumor detection and real-time intraoperative image-guided surgery, which will help to achieve precise removal of the cancer.[22]

Simple Overview of UCNPs

Up-conversion luminescence is a process of luminescent substances absorbing long-wavelength radiation while emitting short-wavelength radiation, and a different luminescence from traditional photoluminescence. The unique luminescent mechanism of UCNPs provides premier optical properties and prospects for widespread applications.

Luminescent Mechanisms of UCNPs

Trivalent lanthanide ions are filled with 4f energy levels without being affected by crystal field and ligand field, because of the shielding of $5S^2$ and $5P^6$ electronic shells. The RE ions can produce a specific up-conversion luminescence (UCL) when electrons jump between 4f energy levels. UCL is a unique photoluminescence compared to down-conversion, because it converts near-infrared long-wavelength excitation into short and visible wavelengths. The working mechanism of UCL has six different categories: excited state absorption (ESA); energy transfer upconversion (ETU); photon avalanche (PA); two photon absorption excitation (TPA); cooperative sensitization (CS) and cooperative luminescence (CL). This review focuses on three main classes (ESA, ETU and PA), which are all involved in the sequential absorption of two more photons. The ESA process is necessary for UCL, which requires the sequential absorption of pump photons by lanthanide ion (Figure 1A).[23] The ETU shares similarity with ESA, moreover, the excitation energy derived from the two neighboring ions transfer can absorb energy from a pump photon (Figure 1B). The PA process can be regarded as a combined process of ESA and ETU, in contrast the energy transfer occurring between the same ions requires a pump intensity above a threshold value; otherwise, the UCL intensity will be very weak. The energy diagram of the PA process is shown in Figure 1C. The other three categories of UCL processes (TPA, CS and CL) are shown in Figure 1D–F.

Components of UCNPs

Inorganic substrates, activator ions and sensitizer ions are indispensable components of RE UCNPs. The up-conversion luminescence approach works with many inorganic substrates, including halides, oxides, sulfides, and inorganic salts. An ideal substrate (eg, fluorides) should have higher chemical stability and lower photon energy of the crystal lattice.[24] Activator ions referred to as doped RE trivalent ions (such as Er^{3+}, Tm^{3+}, Ho^{3+}, Tb^{3+}, and Dy^{3+}) act as efficient luminescence centers.[25,26] The sensitizer ions can improve luminescent performance and are involved in energy transfer. Yb^{3+}, Ce^{3+}, Ho^{3+} and Gd^{3+} are well-known sensitizer ions for lanthanide-related up-conversion emission. Yb^{3+} has a photon absorption at 980 nm, and it's also the most commonly used activator for
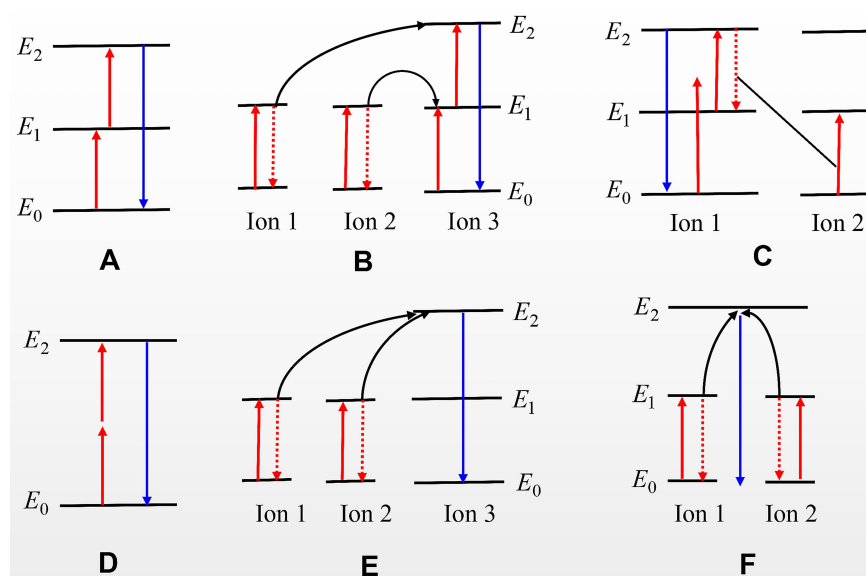
Figure 1 Several energy-transfer mechanisms of UCL process. (**A**) ESA; (**B**) ETU; (**C**) PA; (**D**) TPA; (**E**) CS; (**F**) CL. Red arrows represent the excitation light; blue arrows represent the up-conversion emission.

enhancing luminous efficiency. Doped Yb^{3+} can greatly enhance the luminous efficiency and produce different wavelengths of light by multiplex doping, including Yb^{3+} co-doped with Tm^{3+} and Er^{3+} (shown in Figure 2).

Factors That Influence the Quantum Yield and Emission Color

The luminescent process of UCNPs could be affected by many factors, including the choice of substrates, activators

Figure 2 The energy transfer mechanisms of the up conversion processes in sensitizer Yb^{3+} crystals codoped activator Tm^{3+} and Er^{3+} under 980 nm diodelaser excitation. The photon excitation, energy transfer, multi-photon relaxation and emission processes are shown as dashed-dotted, dashed, dotted and full arrows respectively. Only visible and NIR emissions are shown here. (Based on ideas from Wang F, Liu X. Recent advances in the chemistry of lanthanide-doped upconversion nanocrystals. *Chem Soc Rev.* 2009;38:976–989. doi:10.1039/b809132n.[23]

and sensitizers, temperature, and other substances' interference. There are still challenges for further improving the luminescent efficiency. The absolute quantum yield (QY) is often used to evaluate the luminescent efficiency of different UCNPs. The QY was defined as the ratio of photons emitted and photons absorbed, expressed as QY%=L_{sample}/($E_{reference}$-E_{sample}), where L_{sample} represents emission intensity. $E_{reference}$ and E_{sample} respectively represent the excitation-light intensities that not absorbed by sample and reference sample.[27] The QY% value is often less than 50%, because luminescence needs to absorb at least two photons with emitting one photon. There were three different ways used to improve QY% of UCNPs; including use of appropriate crystalline phases and substrates, constructing core-shell structures, and creating surface plasmon-coupled emission (SPCE).[28] Different activators can emit multiple emission bands (displayed in purple, blue, green, red and near-infrared spectra). There are different ways to achieve color-controllable up-conversion emission, including regulation of doped ions, crystalline phase control and structural modification.[29–31]
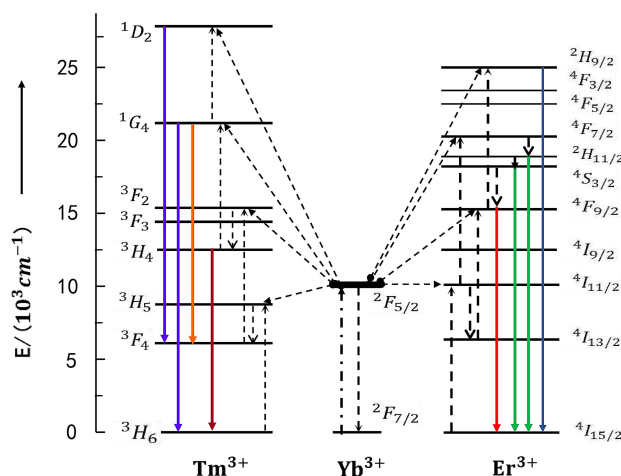
Synthesis and Surface Functionalization of UCNPs

UCNPs can be successfully synthesized by many methods, such as the sol-gel method, co-precipitation, the microemulsion-mediated process, the hydrothermal/solvothermal route, thermal decomposition and so on. Each method has its advantages and disadvantages. Recently, the

co-precipitation method is the most widely used method, which utilizes the precipitation reaction of positive and negative ions in a homogeneous solution to obtain uniformly precipitated UCNPs. Li et al[32] constructed $NaLnF_4$ UCNPs by high-temperature coprecipitation (305 °C) and simultaneously modified size, phase and UCL properties of UCNPs by doping nonequivalent $M^{2+}(Mg^{2+}, Co^{2+})$. The results showed that the prepared UCNPs had small size, hexagonal phase structure and obvious UCL enhancement.[32] However, the size and morphology of the products prepared in the precipitation reaction are uneven and poor. The hydrothermal method mainly utilizes water as the solvent to dissolve and recrystallize powder in the sealed pressure vessel. Compared with other methods, UCNP materials with good crystal phase and uniform particle size can be obtained by using hydrothermal method at lower temperature and lower rare earth salt purity. Wang et al[33] successfully synthesized efficient β-$NaYF_4$:Yb^{3+}, Er^{3+}@β-$NaYF_4$ core/shell nanomaterials via the hydrothermal method in oleylamine solution.[33] Gerelkhuu et al[34] synthesized water-soluble $NaLuGdF_4$:Yb^{3+}/Er^{3+}(Tm^{3+}) nanoparticles with malonic acid (MA) coating via simple one-step hydrothermal method.[34] Moreover, many surface modification methods are also being explored to improve the dispersity of UCNPs in aqueous phase for biomedicine application, including ligand exchange method, polymer coating method and so on. Johnson et al[35] utilized water-soluble polyvinylpyrrolidone (PVP) instead of the passivating oleate ligand on the surface of β-$NaYF_4$ nanoparticles through ligand exchange strategy, and coated the β-$NaYF_4$ nanoparticles with silica shell to prepare highly biocompatible nanoparticles. This method exhibited longer colloidal stability and low aggregation.[35] The functionalized UCNPs used for targeted molecular imaging must have good water solubility and easily bind with target molecules.

Design of Up-Conversion Nanoprobes for Molecular Imaging

Progress has been made for improving UCNPs synthesis, hydrophilic modification and surface functionalization. More importantly, increasing attention has been drawn for exploring their biological application. UCNPs have been used in different molecular tests including cell and whole-body fluorescent imaging (for instance vascular imaging,[36,37] lymph node imaging,[38] and targeted cancer imaging[39]). Previous studies have shown that UCNPs coated with different ligands (silica shells,[40] charged polymers,[41] active small

molecules,[42] biomacromolecules,[43] etc.) and/or covalently linked to functional groups (peptides,[44] folates,[45] antibodies,[46] etc.) can achieve cellular imaging via exocytosis and group-mediated action.[47]

The development of cancer-targeted imaging agents and contrast agents have attracted more of our interest. Rational design of fluorescent probe targeting cancer-specific biomarker is the key. Tumor biomarkers are substances, usually proteins, that are produced specifically in response to cancer developing. There were different biomarkers reported; including carcinoembryonic antigen (CEA),[48] carbohydrate antigen (eg, CA19-9),[49] alpha fetoprotein (AFP),[50] and tumor-associated antigens (eg, prostate-specific membrane antigen, PSMA).[51,52] Tumor-associated antigens are specifically located on cell membrane or in intracellular structure; including epidermal growth factor receptor (EGFR),[53] folate receptor-α (FR-α),[54,55] vascular endothelial growth factor receptor (VEGFR),[56] estrogen receptor (ER), and progesterone receptor (PR). These biomarkers are potential for targeted therapy and imaging of cancer. To obtain the expected imaging effect, it is necessary to modify the UCNP surface to make the probe easier to target and bind with the tumor biomarker. To achieve surface functionalization of UCNPs, different factors affect the outcome including particle size, water solubility, fluorescence efficiency, emission colors, ligand synthesis, and imaging effect.[57]

UCNPs for Cancer Diagnosis
Carboxyl-Functionalized UCNP Probes

UCNP surface within the carboxyl group can bind to ligands within the amino group. Under the action of 1-(3-dimethylaminopropyl)-3-ethylcarbodiimide hydrochloride (EDC) and N-hydroxysulfosuccinimide sodium salt (sulfo-NHS), carboxyl-functionalized UCNPs can bind to different ligands (eg, polyamine, antibodies, avidin, DNA, and folic acid-conjugated chitosan). For instance, $NaYF_4$:Gd, Yb, Er nanoparticles capped by 3-mercaptopropionic acid (3-MPA) can be modified with bio-recognize molecules, including anti-claudin-4 and anti-mesothelin, that further can be used as antibody-functionalized UCNP probe targeting to cancer cells.[58] Kong reported a one-step strategy for synthesis of hydrophilic RE UCNPs using malonic acid as the stabilizer and functional agent.[59] The carboxyl-functionalized UCNPs allowed further conjugation with functional molecules and were also used as fluorescent probes for bioimaging in detecting exonuclease I (Exo I) activity.[59] As shown in Figure 3, the surface of $NaLuF_4$:Yb/Er UCNPs was linked with single-stranded
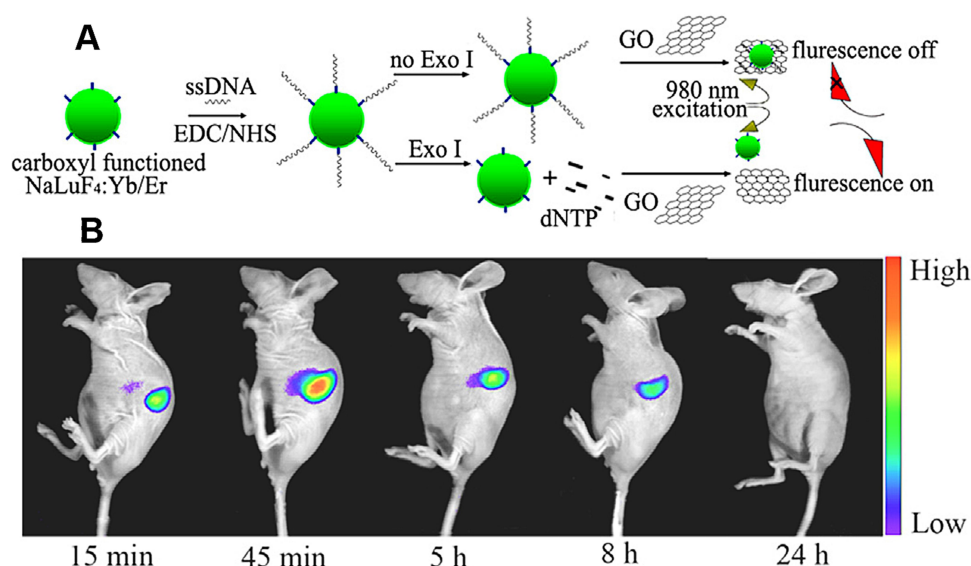
Figure 3 Schematic diagram of the main strategies for the fabrication of carboxyl-functionalized UCNPs nanoprobes. (**A**) Working mechanism of the proposed sensor for Exo I activity detection; (**B**) In vivo NIR luminescence images of a nude mouse after intravenous injection of NaLuF$_4$:Gd/Yb/Tm.
Note: Copyright ©2015. Elsevier B.V. Reproduced from Han G, Li H, Huang X, et al. Simple synthesis of carboxyl-functionalized upconversion nanoparticles for biosensing and bioimaging applications. *Talanta*. 2016;147: 207–212.[59]

DNA (ssDNA), the product absorbed surface of graphene oxide (GO) by the π–π accumulation effect, which achieves the up-conversion luminescence quenching.

Amino-Functionalized UCNP Probes

Amino-functionalized UCNPs could also easily bind to ligands with a carboxyl group (eg, citric acid, polyacrylic acid, oleic acid, DNA, biotin, avidin, antibodies, folic acid, and chlorotoxin). A UCNP surface modified with amino groups can be generated by the link between UCNPs@SiO$_2$ and 3-(trimethoxysilyl)-1-propanamine.[60,61] Yu et al (2010)[62] reported a study of neurotoxin mediated up-conversion nanoprobes for tumor imaging in living animals. The poly-ethylenimine was covalently linked to the surface of synthesized hexagonal-phase NaYF$_4$:Yb, Er/Ce nanoparticles, which can conjugate with recombinant chlorotoxin for specifically binding to glioma cells (Figure 4A). As a result, the fluorescent probe targeted glioma cells can be used for tumor imaging with bright red fluorescence under NIR irradiation (Figure 4B). The synthesized CTX:UCNP nanoprobes also showed strong up-conversion fluorescence and specific binding with tumor cells. Summarizing the whole research, CTX:UCNP nanoprobes administered intravenously with CTX:UCNP nanoprobe can achieve direct visualization of tumors in vivo by strong NIR-to-red up-conversion fluorescence.

Maleimide-Functionalized UCNP Probes

Maleimide-functionalized UCNP probes are often prepared through synthesis of amino-modified UCNPs with bifunctional coupling agents. These probes were used for detecting thiol-containing ligands, including mercaptan, thiophenol, cysteine, glutathione and thiol proteins. Xiong et al (2009)[63] developed up-conversion luminescence (UCL) with high contrast for targeted imaging of tumors, which used RGD-labelled up-conversion nanophosphors (UCNPs) as luminescent labels (shown in Figure 5).

Folic Acid-Functionalized UCNP Probes

There are numerous highly expressed receptors in cancer cells that can specifically bind to different ligands. Folate receptors (FRs), also known as folate-binding proteins (FBPs), were found to be highly expressed in cancer tissues compared to adjacent normal tissues.[64] This finding was shown in myeloid leukemia, mesothelioma, and different sites of cancer including endometrial, lung, ovarian, breast, kidney, and brain.[64] Folate with conjugates can enter into cells via receptor-mediated endocytosis. They can be used for folate-targeted imaging and also be used as therapeutic agents specific to FR-expressing tumors.[65,66] Amino-functionalized UCNPs can be easily functionalized with folic acid to form UCNPs-NH$_2$-FA, which can be internalized into cancer cells efficiently and used for up-conversion luminescent sensing and bioimaging.[67]
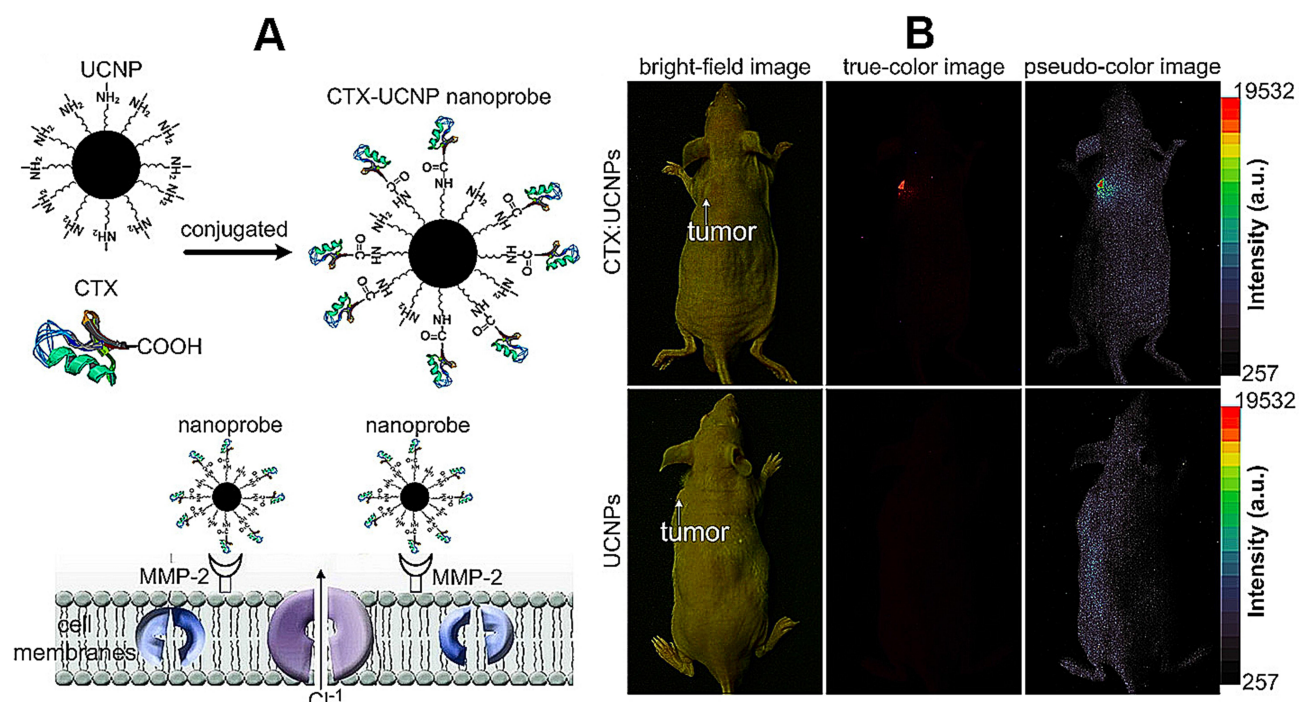
Figure 4 Fabricating and imaging of amino-functionalized UCNPs probes. (**A**) Preparation and specific glioma cell binding of CTX-UCNPs probes; (**B**) In vivo tumor imaging of a representative Balb-c nude mouse after intravenous injection of CTX:UCNPs (top) or unconjugated UCNPs (bottom) for 24 hours.
Note: Copyright ©2010. Elsevier Ltd. Reproduced from Yu XF, Sun Z, Li M, et al. Neurotoxin-conjugated upconversion nanoprobes for direct visualization of tumors under near-infrared irradiation. *Biomaterials*. 2010;31: 8724–8731.[62]
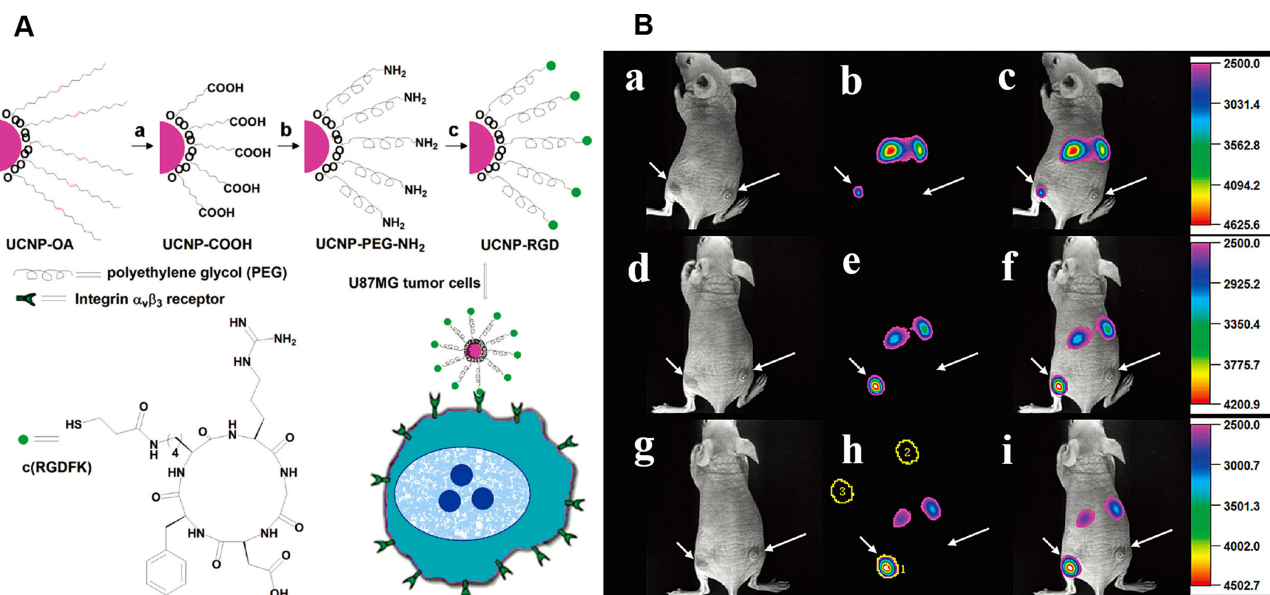

Figure 5 Illustration scheme for UCNP-RGD (**A**) and in vivo up-conversion luminescence imaging of subcutaneous U87MG tumor (left hind leg) and MCF-7 tumor (right hind leg) after intravenous injection of UCNP-RGD conjugate over a 24-hour period (**B**). (a, d, g) bright field, (b, e, h) up-conversion images, (c, f, i) overlay of the corresponding bright field images with the up-conversion ones. (a–c), (d–f), and (g–i) are taken at 1, 4 and 24 hours postinjection, respectively.
Note: Copyright ©2009. American Chemical Society. Reproduced from Xiong L, Chen Z, Tian Q, et al. High contrast upconversion luminescence targeted imaging in vivo using peptide-labeled nanophosphors. *Anal Chem*. 2009;81: 8687–8694.[63]

UCNP Probes for Dual-Modal and Multi-Modal Cancer Imaging

Molecular imaging has been highly developed; X-ray computed tomography (X-CT), magnetic resonance imaging (MRI), single-photon emission computed tomography (SPECT), positron emission tomography (PET), and ultrasound (eg, ultrasound contrast imaging, UCI) are commonly used in clinical practice. With the development of infrared fluorescence probes, optical molecular imaging (OMI) has been successfully used in living animals. Notably, every imaging technique has advantages and limitations in relation to imaging objects, spatial resolution, imaging depth and maximum sensitivity. For instance, CT and MRI are unable to be used at the cellular level. OMI has high resolution and sensitivity for imaging at the cellular level, but it cannot provide three-dimensional imaging of tissue. High-resolution imaging of both tissues and cells can be achieved by combining OMI with CT and MRI. Dong et al[68] (2019) synthesized $ZnFe_2O_4$ nano-material with excellent performance of MRI/OMI/CT tri-modal imaging, low toxicity and no fluorescence quenching has also been reported. Developing UCNP probes with multi-modal imaging would be necessary and useful. The UCNP probes for multi-modal imaging may integrate advantages of different imaging modalities, which further supports the development of accurate diagnosis and guided therapy in the near future.[69]

UCNPs as Phototherapeutic Reagents

Photodynamic Therapy (PDT)

Photodynamic therapy (PDT) makes use of reactive oxygen species (ROS) generated by photosensitizers that kill malignant cells by apoptosis or necrosis, which further suppress tumor microvasculature and stimulate the host immune response.[70] However, conventional PDT has limited tissue-penetration depth (<1 cm), and it can only be used for treatment of flat lesions. The most promising use of PDT is deep penetration by NIR-excitable UCNPs that can penetrate thick tissue. UCNP surface modification and connection with an organic photosensitizer need to be considered for rational design. Photosensitizer with high ROS production, high absorption coefficient for tissue penetration, amphiphilicity, low dark toxicity, ease of synthesis, and ease of formulation in aqueous solvent for in-vivo delivery were all needed for qualified PDT.[71] Commonly used photosensitizers with PDT can be classified into porphyrin, chlorin, phthalocyanine, naphthalocyanine and 5-amino-levulinic acid. Clinically approved photosensitizers, including temoporfin, verteporfin, porfimer sodium, temoporfin, methyl aminolevulinate, talaporfin sodium, and aluminium phthalocyanine disulfonate, provided different options.[72] There are three different pathways of localizing photosensitizers onto UCNPs for PDT: silica encapsulation, physical adsorption and covalent conjugation. UCNPs have been reported as drug nanocarriers and electron donors that effectively access deep tumors,[73] which further facilitate both in-vitro and in-vivo cancer cell killing through low red irradiation. Professor Han's group (Punjabi et al.[73]) developed a class of bio-compatible UCNPs with amplified red emissions.[73] Synthesized UCNP-PDT showed a high up-conversion quantum yield (3.2% in red emission), which is 15-fold stronger than well-known optimal β-phase core/shell UCNPs. When conjugated to amino-levulinic acid, significant PDT effect in tumor was observed in deep tissue (>1.2 cm) in vivo under bio-compatible laser power. In 2020, Liu et al[74] reported synthesized nanostructures (Nd^{3+}-sensitized) of up-conversion metal organic frameworks (MOFs), which can be used for mitochondria-targeted amplified PDT. Under excitation of 808-nm NIR, Nd^{3+}-sensitized up-conversion MOFs captured low-energy photons and delivered energy to MOF domain by efficient resonance energy transfer. This process specifically generated ROS in mitochondria to complete PDT. In addition, 808 nm excitation can improve safety of laser applications. Because traditional 980 nm excited up-conversion luminescence could cause damage to normal tissues through thermal effect. Despite many advantages of using UCNPs for bio-compatible photodynamic therapy, deep-tissue therapy via UCNPs still needs to overcome challenges.

Photothermal Therapy (PTT)

Similar to PDT, PTT is another promising choice for oncological treatment with minimal invasion. PTT uses light energy to induce localized heat within tissue and then destroy pathologic cells. UCNP-based PDT and PTT have advanced development due to advantages of no surgery required and no damage to healthy tissues, compared to conventional chemotherapy, radiotherapy and surgery. Typical photothermal agents contain heavy metals (eg, gold, silver, palladium, platinum),
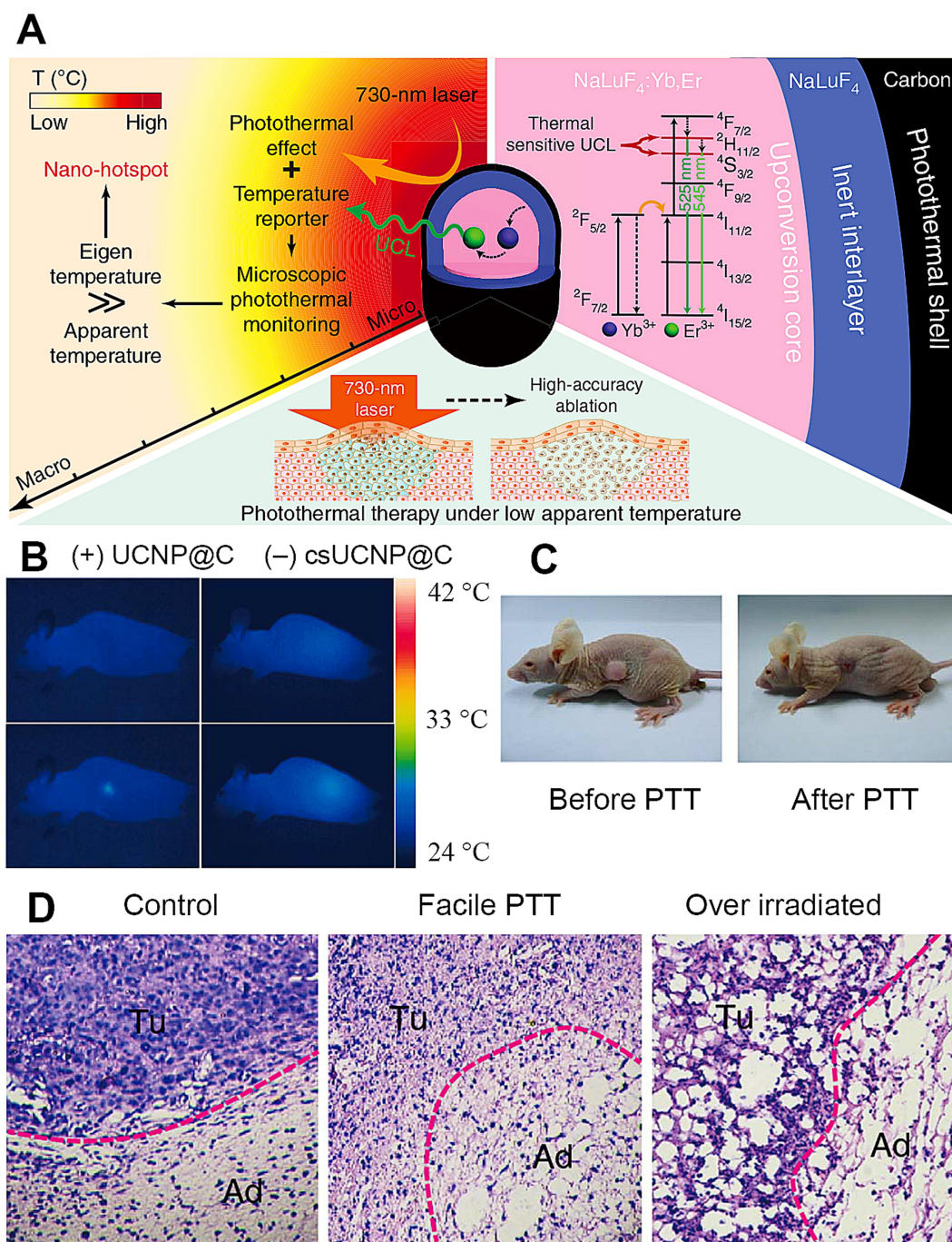
Figure 6 (**A**) Working principle of csUCNP@C nanocomposite for high-accurate PTT at facile temperature. (**B**) Thermal images of nude mice with (left panel) and without (right panel) csUCNP@C-labelled HeLa cell tumors. (**C**) Representative photos of nude mice transplanted with csUCNP@C-labelled HeLa cells. (**D**) H&E stained tumor sections of the border of tumor and normal fat tissue. The tumor region (Tu) and the adipocytes (Ad) in normal fat tissue of the mice without irradiation (left, Control) is compact and the tumor cells are stretched. Following photothermal treatment (middle, Facile PTT), the tumor region became loose and fragile and the tumor cells are atrophic. The adipocytes (Ad) in normal fat tissue are intact with minimal damage. However, following high-power irradiation, both Tu and Ad suffered extreme damage (right, Over irradiated). All irradiation processes were under 730-nm and 0.3 Wcm^{-2} except high-power (0.8 Wcm^{-2}). Reproduced from Zhu X, Feng W, Chang J, et al. Temperature-feedback upconversion nanocomposite for accurate photothermal therapy at facile temperature. *Nat Commun*. 2016;7:10437. creative commons license and disclaimer available from: http://creativecommons.org/licenses/by/4.0/legalcode"http://creativecommons.org/licenses/by/4.0/legalcode.[75]

semiconductors (eg, copper sulphide, copper selenide), dye (eg, prussian blue, indocyanine green), conjugated polymer (eg, polypyrrole, polyaniline) and carbon-based nanomaterial (eg, graphene, carbon nanotubes). In 2016, Zhu et al[75] synthesized a carbon-coated core-shell up-conversion nanocomposite: $NaLuF_4$:Yb, $Er@NaLuF_4$

@Carbon also called csUCNP@C, which facilitated accurate PTT by real-time monitoring of microscopic temperature (shown in Figure 6). In the presence of suitable UCNP probes and contrast agents, multi-modal imaging and therapy can be integrated for an accurate image-guided cancer diagnosis and treatment.[76]

UCNP Probes for Detecting Tumor Microenvironment

Due to metabolic differences between normal and cancer cells, features including highly expressed matrix metalloprotease (MMP), high ROS level, hypoxia, low pH, over-expressed folate receptor, and enhanced permeability and retention (EPR) were reported in the tumor microenvironment (TME). Proteases functionalized in diverse cellular processes, including cell growth, division, differentiation, migration, and signal transduction, excluding protein turnover. Normal cells have the metabolic balance between protease activation and inhibition, and imbalance of protease is closely related to pathogenesis and progression of cancers. MMPs are often highly expressed in both the extracellular environment and in cancer cells, which contributes to extracellular matrix remodeling and cancer metastasis. ROS was found that promoted tumor occurrence and development, and also contributed to tumor-induced immunosuppression.[77] The ROS level in tumor cells was correlated with activity of signal transducer and activator of transcription 3/5 (STAT3/5), which were found activated in many tumor cells.[78] Activated glycolysis in cancer cells could lead to accumulation of lactic acid in TME, and many carboxylate transporters were also over-expressed on the surface of cancer cells.[13] Moreover, tumorigenesis also led to a hypoxic environment,[79] over-expressed folate receptors[80,81] and the EPR effect.[82,83] There are outstanding achievements by utilizing UCNP probes for cancer diagnosis and treatment based on the specific features of TME. Protease-activated probes,[84] pH-sensitive probes[85–87] and hypoxia-responsive probes[88–90] have been reported. Li et al[91] (2018) developed the pH-sensitive photodynamic nanomaterials (PPNs) composed of photosensitizers (PS) grafted ligands (pH-responsive polymer) and UCNPs. Under neutral pH (pH = 7.4), the negative charged PPNs could be self-quenched. Under mildly acidic TME (pH = 6.5), PPNs efficiently enhanced cellular internalization and then transferred to single UCNP in lysosomes (pH = 5.5), which efficiently enabled the activation of PS. Upon NIR irradiation, the UCL from

PPNs can induce the photoactivity of free PS in acidic TME to kill tumor cells. In 2019, Liu et al[92] reported a smart image-guided diagnostic and therapeutic nanoplatform by modifying polyoxometalate (POM) nanoclusters onto mesoporous silica-coated UCNPs (NaYF$_4$:Yb, Er@NaYF$_4$:Yb, Nd). Subsequently, Liu's group loaded doxorubicin (DOX) in mesopores and coated a folate-chitosan shell onto the surface. In relation to the EPR effect, the nanoplatform can achieve dual-modal (OMI and CT) imaging and produce heat as an efficient synergistic therapy path (shown in Figure 7). This study highlighted utilization of UCNPs by TME-specificity mediated diagnosis and therapy.

Actually, there are a great many researches focused on the application of UCNPs on cancer medicine. Due to the unique features of nanotechnology applied in oncology (eg, more sensitive cancer diagnosis and imaging, co-delivery of multiple drugs to improve therapeutic efficacy and delivery of appropriate drug ratio to the target of interest),[93] more and more new types of UCNPs were designed and studied to develop more accurate imaging, more effective nanotherapeutics and more sensitive diagnosis for cancer. Some correlational researches on UCNPs-based nanosystem for tumor phototheranostics[90,94–97] are illustrated in Table 1. With the intensive study and rapid development of UCNPs and tumor markers, we believe that using lanthanide-based UCNPs co-carrying anti-tumor drug and sensitizer to reach the integration of cancer molecular imaging, diagnosis and treatment are not unrealistic aims for the near future.

Nano-Toxicity of UCNPs in vitro and in vivo

UCNPs could be widely used in biosensor, biological imaging, and tumor therapy. However, there are also risks for causing nano-toxicity in human cells, tissues, and organs.[98] Therefore, studies need to be performed to characterize in-vitro cytotoxicity and long-term toxicity in vivo.[99] UCNPs are usually modified by surface coating, including polyvinylpyrrolidone (PVP), polyethylenimine (PEI) and SiO$_2$,[47] which generate UCNPs with stability, safety and biocompatibility. There are well used methods for detecting in-vitro cytotoxicity of UCNPs, including MTT, MTS and CCK-8 assays. Functionalized water-soluble UCNPs with well-defined concentration and incubation time, caused very low cytotoxicity in Hela, glioma U87MG and MCF-7 cells.[99,100] Moreover, it is necessary
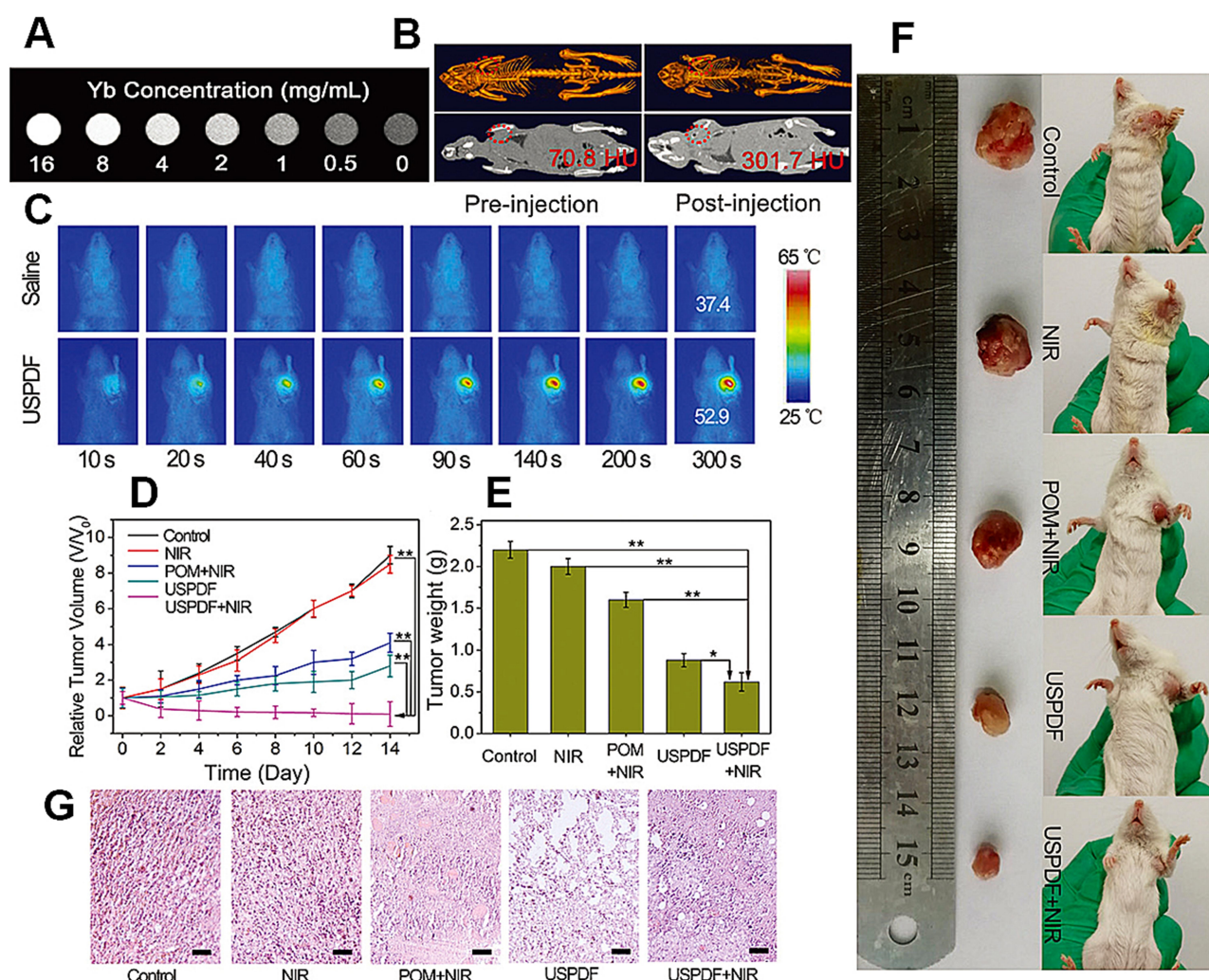
Figure 7 (A) In vitro CT images of USPDF (ie, prepared UCNPs@mSiO$_2$-POM-DOX@FC) at different Yb concentrations. **(B)** In vivo CT images of tumor-bearing mice before and after USPDF injection. **(C)** Photothermal images of tumor-bearing mice after injecting saline and USPDF under 808 nm laser irradiation for different times. **(D)** Changes in relative tumor volume. **(E)** Tumor weight at the 14th day of each group. **(F)** Photographs at the 14th day of representative tumors collected from different groups. **(G)** H&E histologic section of tumor collected from different groups of mice after 14 day treatment, scale bars are 50 μm. The statistical significance in different groups was analyzed using t-test, *p < 0.05 and **p < 0.01.
Note: Copyright ©2018. The Royal Society of Chemistry. Reproduced from Liu S, Li W, Gai S, et al. A smart tumor microenvironment responsive nanoplatform based on upconversion nanoparticles for efficient multimodal imaging guided therapy. Biomater Sci. 2019;7: 951–962.[92]

to evaluate long-term toxicity and biodistribution of UCNPs through using in-vivo models. To date, toxicity assessment of UCNPs have been carried out in *Caenorhabditis elegans* (*C. elegans*), zebrafish, and mice.[101–104] The results suggested that delivery of UCNPs by feeding showed less toxicity in both *C. elegans* and zebrafish. The most reported delivery of UCNPs into living mice were focused on intravenous injection, and UCNPs could be accumulated in reticuloendothelial systems.[105] In 2011, Cheng et al[106] studied the potential toxicity of UCNPs functionalized by PAA and PEG. There were residual UCNPs left in liver and spleen

of mice for 3 months without obvious toxicity identified. The UCNPs accumulation in tumor can be improved by targeted modification. Wang et al (2020)[103] reported UNCPs (NaYF$_4$: Yb, Tm) coated with cancer cell membrane as a probe for improving the biocompatibility and ability of immune escape.[107,108] Chu et al (2019)[108] reported an activatable engineered immunodevice (composed of a rationally designed UV light-activatable immunostimulatory agent and UCNPs) that enables remote control over the antitumor immunity in vitro and in vivo with near-infrared (NIR) light. The controlled immune regulation allows the generation of effective immune

Table 1 Summary of UCNPs-Based Nanosystem for Cancer Imaging and Phototheranostics

UCNPs	Coating	Cargo/Drug	Imaging Modality Type Modality	Therapy Type	Cell	Refs.
NaGdF$_4$:Yb, Tm@NaGdF$_4$:Yb	ZnFe$_2$O$_4$	DOX	OMI, MRI, CT	PDT, CDT, chemotherapy	HeLa	[68]
NaGdF$_4$:Yb, Er@NaGdF$_4$:Yb, Nd	–	–	–	PDT	4T1	[74]
NaLuF$_4$:Yb, Er@NaLuF$_4$	Carbon	–	–	PTT	HeLa	[75]
NaYF$_4$:Yb, Er@CaF$_2$:Yb(80%), Er(2%)@CaF2	–	Ce6	OMI	PDT	HepG2	[91]
NaYF$_4$:Yb, Er@NaYF$_4$:Yb, Nd	SiO$_2$	DOX	OMI, CT	PTT, chemotherapy	HeLa	[92]
NaYF$_4$:Yb, Tm@NaGdF$_4$:Yb	TiO$_2$	–	MRI, CT	PDT	HeLa	[94]
NaYF$_4$:Er, Yb	PLGA/Span 80/Cremophor A25	Rose bengal	–	PDT	MeWo/Me-45	[95]
NaYF$_4$:Er, Yb	PEG	Rose bengal	–	–	–	[96]
NaGdF$_4$:Yb, Er @ NaGdF$_4$:Yb	MnO$_2$/SiO$_2$/PEG	DOX, Ce6	MRI, CT	Chemotherapy, PDT	HeLa, U14	[90]
NaYF$_4$:Yb, Er, Gd@NaYF$_4$	Lysine	Rose bengal	–	PDT	SK-BR-3	[97]
NaYF$_4$: Yb, Tm	Cell membrane	GOX	–	PTT, starvation therapy	4T1	[103]

response within tumor without disturbing immunity elsewhere in the body, thereby maintaining the antitumor efficacy while mitigating systemic toxicity.

Conclusions and Prospects

This review of up-conversion luminescence demonstrates that UCNPs are different from conventional dyes and nanomaterials regarding their optical performance. Many studies have reported remarkable features of UCNPs, including unique fluorescent stability, strong organizational penetration, auto-fluorescence-free background and low bio-system interference in the NIR region. As a result, UCNPs have shown great prospects of utilization in diagnosis and treatment of cancer. In addition, UCNPs can be easily synthesized and functionalized. For cancer imaging and diagnosis, functionalized UCNP probes can be designed based on distinguishable properties of cancer cells through diverse surface modification and functionalization. At present, researchers aim to improve the sensitivity and selectivity of those probes for visualized diagnosis and therapy of tumors.[1] NIR fluorescent imaging showed a number of advantages compared with conventional imaging by UV-visible optical spectrum. However, NIR imaging can only detect superficial and shallow-seated tumors, and is unable to explore the internal structure of tumors. Multi-modal imaging can detect different targets simultaneously through sophisticated design of UCNP probes, which resolve problems by a single modal and accurately provided guide in cancer surgery. In recent years, the progress has been made to improve sensitivity of probes for diagnostic purposes. It's reasonable to believe that UCNPs can be successfully used in early diagnosis and image-guided surgery of cancer in the near future. In addition, both PDT and PTT are important non-invasive surgical treatments. It can be further developed for application of UCNPs in PDT and PTT. These pre-clinical UCNP probes also need to be well studied for safety assessments and clinical validations. Multi-disciplinary collaboration between chemists, biologists, engineers, and surgeons will greatly contribute to developing UCNPs to form integrated models of cancer diagnosis and treatment.

Acknowledgments

Disclosure

The authors report no conflicts of interest in this work.

References

1. Li ZH, Yuan H, Yuan W, et al. Upconversion nanoprobes for biodetections. *Coord Chem Rev.* 2018;354:155–168. doi:10.1016/j.ccr.2017.06.025
2. Yang YM, Han Y, Yue CX. Up-conversion nanoparticles for gastric cancer targeted imaging and therapy. *Nano Biomed Eng.* 2016;8:161–171. doi:10.5101/nbe.v8i3.p161-171
3. Zhou B, Shi BY, Jin DY, Liu XG. Controlling upconversion nanocrystals for emerging applications. *Nat Nanotechnol.* 2015;10:924–936. doi:10.1038/nnano.2015.251
4. Yang DM, Ma P, Hou ZY, et al. Current advances in lanthanide ion (Ln^{3+})-based upconversion nanomaterials for drug delivery. *Chem Soc Rev.* 2015;44:1416–1448.
5. Haase M, Schafer H. Upconverting nanoparticles. *Angew Chem Int Ed.* 2011;50:5808–5829.
6. Wu RT, Zhan QQ, Liu HC, et al. Optical depletion mechanism of upconverting luminescence and its potential for multi-photon STED-like microscopy. *Opt Express.* 2015;23:32401–32412. doi:10.1364/OE.23.032401
7. Deng M, Wang L. Unexpected luminescence enhancement of upconverting nanocrystals by cation exchange with well retained small particle size. *Nano Res.* 2014;7:782–793.
8. Patra JK, Das G, Fraceto LF, et al. Nano based drug delivery systems: recent developments and future prospects. *J Nanobiotechnol.* 2018;16:71–103.
9. Bray F, Ferlay J, Soerjomataram I, et al. Global cancer statistics 2018: GLOBOCAN estimates of incidence and mortality worldwide for 36 cancers in 185 countries. *CA Cancer J Clin.* 2018;68:394–424. doi:10.3322/caac.21492
10. Kahi CJ, Boland CR, Dominitz JA, et al. Colonoscopy surveillance after colorectal cancer resection: recommendations of the US multi-society task force on colorectal cancer. *Gastroenterology.* 2016;150:758–768. doi:10.1053/j.gastro.2016.01.001
11. Wasif N, Etzioni D, Habermann EB, et al. Racial and socioeconomic differences in the use of high-volume commission on cancer-accredited hospitals for cancer surgery in the United States. *Ann Surg Oncol.* 2018;25:1116–1125. doi:10.1245/s10434-018-6374-0
12. Jaffray DA, Das S, Jacobs PM, et al. How advances in imaging will affect precision radiation oncology. *Int J Radiat Oncol Biol Phys.* 2018;101:292–298.
13. Wang C, Wang Z, Zhao T, et al. Optical molecular imaging for tumor detection and image-guided surgery. *Biomaterials.* 2018;157:62–75. doi:10.1016/j.biomaterials.2017.12.002
14. Weissleder R. Molecular imaging: exploring the next frontier. *Radiology.* 1999;212:609–614. doi:10.1148/radiology.212.3.r99se18609
15. Toczek J, Sadeghi MM. Molecular imaging concepts. *J Nucl Cardiol.* 2016;23:271–273. doi:10.1007/s12350-016-0403-9
16. Fujibayashi Y. Concept of molecular imaging. *Nihon Rinsho Jpn J Clin Med.* 2007;65:199–203.
17. Hussain T, Nguyen QT. Molecular imaging for cancer diagnosis and surgery. *Adv Drug Deliv Rev.* 2014;66:90–100. doi:10.1016/j.addr.2013.09.007
18. Jiang Q, Liu Y, Guo R, et al. Erythrocyte-cancer hybrid membrane-camouflaged melanin nanoparticles for enhancing photothermal therapy efficacy in tumors. *Biomaterials.* 2019;192:292–308. doi:10.1016/j.biomaterials.2018.11.021
19. Gao S, Yang DJ, Fang Y, et al. Engineering nanoparticles for targeted remodeling of the tumor microenvironment to improve cancer immunotherapy. *Theranostics.* 2019;9:126–151. doi:10.7150/thno.29431
20. Jia F, Li G, Yang B, et al. Investigation of rare earth upconversion fluorescent nanoparticles in biomedical field. *Nanotechnol Rev.* 2019;8:1–17. doi:10.1515/ntrev-2019-0001
21. Naczynski DJ, Tan MC, Riman RE, et al. Rare earth nanoprobes for functional biomolecular imaging and theranostics. *J Mater Chem B.* 2014;2:2958–2973. doi:10.1039/C4TB00094C
22. Mondal SB, Gao S, Zhu N, et al. Real-time fluorescence image-guided oncologic surgery. *Adv Cancer Res.* 2014;124:171–211.
23. Wang F, Liu X. Recent advances in the chemistry of lanthanide-doped upconversion nanocrystals. *Chem Soc Rev.* 2009;38:976–989. doi:10.1039/b809132n
24. Liang X, Wang X, Zhuang J, et al. Synthesis of NaYF$_4$ nanocrystals with predictable phase and shape. *Ad? Funct Mater.* 2007;17:2757–2765. doi:10.1002/adfm.200600807
25. Loo C, Chien YH, Yin F, et al. Upconversion and downconversion nanoparticles for biophotonics and nanomedicine. *Coord Chem Rev.* 2019;400:213042. doi:10.1016/j.ccr.2019.213042
26. Boyer JC, Cuccia LA, Capobianco JA, et al. Synthesis of colloidal upconverting NaYF$_4$: er^{3+}/Yb^{3+} and Tm^{3+}/Yb^{3+} monodisperse nanocrystals. *Nano Lett.* 2007;7:847–852.
27. Boyera JC, Veggel F. Absolute quantum yield measurements of colloidal NaYF$_4$: er^{3+}, Yb^{3+} upconverting nanoparticles. *Nanoscale.* 2010;2:1417–1419. doi:10.1039/c0nr00253d
28. Bulíř J, Zikmund T, Novotný M, et al. Photoluminescence excitation of lithium fluoride films by surface plasmon resonance in Kretschmann configuration. *Appl Phys A.* 2016;122:412. doi:10.1007/s00339-016-9971-4
29. Deng R, Qin F, Chen R, et al. Temporal full-colour tuning through non-steady-state upconversion. *Nat Nanotechnol.* 2015;10:237–242. doi:10.1038/nnano.2014.317
30. Pei WB, Chen B, Wang L, et al. NaF-mediated controlled-synthesis of multicolor Na$_x$ScF$_{3+x}$: yb/Erupconversion nanocrystals. *Nanoscale.* 2015;7:4048–4054. doi:10.1039/C4NR06637E
31. Wen H, Zhu H, Chen X, et al. Upconverting near-infrared light through energy management in core-shell-shell nanoparticles. *Angew Chem Int Ed.* 2013;52:13419–13423. doi:10.1002/anie.201306811
32. Li Y, Li X, Xue Z, et al. M^{2+} doping induced simultaneous phase/size control and remarkable enhanced upconversion luminescence of NaLnF$_4$ probes for optical-guided tiny tumor diagnosis. *Adv Healthc Mater.* 2017;6:161231. doi:10.1002/adhm.201601231
33. Wang Y, Tu L, Zhao J, et al. Upconversion luminescence of β-NaYF$_4$: yb^{3+}, Er^{3+}@β-NaYF$_4$ core/shell nanoparticles: excitation power density and surface dependence. *J Phys Chem C.* 2009;113:7164–7169. doi:10.1021/jp9003399
34. Gerelkhuu Z, Huy B, Sharipov M, et al. One-step synthesis of NaLu$_{80-x}$Gd$_x$F$_4$: yb$_{18}^{3+}$/Er$_2^{3+}$(Tm^{3+}) upconversion nanoparticles for in vitro cell imaging. *Mater Sci Eng C Mater.* 2017;86:56–61. doi:10.1016/j.msec.2017.11.019
35. Johnson N, Sangeetha N, Boyer J, et al. Facile ligand-exchange with polyvinylpyrrolidone and subsequent silica coating of hydrophobic upconverting β-NaYF$_4$:Yb^{3+}/Er^{3+}nanoparticles. *Nanoscale.* 2010;2:771–777. doi:10.1039/b9nr00379g

36. Qiao R, Qiao H, Zhang Y, et al. Molecular imaging of vulnerable atherosclerotic plaques in vivo with osteopontin-specific upconversion nanoprobes. *ACS Nano*. 2017;11:1816–1825. doi:10.1021/acsnano.6b07842

37. Xue Z, Zeng S, Hao J, et al. Non-invasive through-skull brain vascular imaging and small tumor diagnosis based on NIR-II emissive lanthanide nanoprobes beyond 1500 nm. *Biomaterials*. 2018;171:153–163. doi:10.1016/j.biomaterials.2018.04.037

38. Qiu S, Zeng J, Hou Y, et al. Detection of lymph node metastasis with near-infrared upconversion luminescent nanoprobes. *Nanoscale*. 2018;10:21772–21781. doi:10.1039/C8NR05811C

39. Rao L, Bu LL, Cai B, et al. Cancer cell membrane-coated upconversion nanoprobes for highly specific tumor imaging. *Adv Mater*. 2016;28:3460–3466. doi:10.1002/adma.201506086

40. Song X, Yue Z, Hong T, et al. Sandwich-structured upconversion nanoprobes coated with a thin silica layer for mitochondria-targeted cooperative photodynamic therapy for solid malignant tumors. *Anal Chem*. 2019;91:8549–8557. doi:10.1021/acs.analchem.9b01805

41. Ma Y, Ji Y, You M, et al. Labeling and long-term tracking of bone marrow mesenchymal stem cells in vitro using NaYF$_4$: yb^{3+}, Er^{3+} upconversion nanoparticles. *Acta Biomater*. 2016;42:199–208. doi:10.1016/j.actbio.2016.07.030

42. Kong W, Sun T, Chen B, et al. A general strategy for ligand exchange on upconversion nanoparticles. *Inorg Chem*. 2017;56:872–877. doi:10.1021/acs.inorgchem.6b02479

43. Lu J, Chen Y, Liu D, et al. One-step protein conjugation to upconversion nanoparticles. *Anal Chem*. 2015;87:10406–10413. doi:10.1021/acs.analchem.5b02523

44. Yao C, Wei C, Huang Z, et al. Phosphorylated peptide functionalization of lanthanide upconversion nanoparticles for tuning nanomaterial-cell interactions. *ACS Appl Mater Interfaces*. 2016;8:6935–6943. doi:10.1021/acsami.6b01085

45. Huang M, Wang LJ, Zhang XJ, et al. Synthesis and characterization of folic acid labeled upconversion fluorescent nanoprobes for in vitro cancer cells targeted imaging. *Nano*. 2017;12:1750057. doi:10.1142/S1793292017500576

46. He H, Howard CB, Chen Y, et al. Antibody-functionalized upconversion nanoprobe. *Anal Chem*. 2018;90:3024–3029. doi:10.1021/acs.analchem.7b05341

47. Jin J, Gu YJ, Man CW, et al. Polymer-coated NaYF$_4$: yb^{3+}, Er^{3+} upconversion nanoparticles for charge-dependent cellular imaging. *ACS Nano*. 2011;5:7838–7847. doi:10.1021/nn201896m

48. Wang Y, Wei Z, Luo X, et al. An ultrasensitive homogeneous aptasensor for carcinoembryonic antigen based on upconversion fluorescence resonance energy transfer. *Talanta*. 2019;195:33–39. doi:10.1016/j.talanta.2018.11.011

49. Thomsen M, Skovlund E, Sorbye H, et al. Prognostic role of carcinoembryonic antigen and carbohydrate antigen 19-9 in metastatic colorectal cancer: a *BRAF*-mutant subset with high CA 19-9 level and poor outcome. *Br J Cancer*. 2018;118:1609–1616. doi:10.1038/s41416-018-0115-9

50. Chen X, Xu W, Jiang Y, et al. Near-infrared-light-triggered photoelectrochemical biosensor for detection of alpha-fetoprotein based on upconversion nanophosphors. *Nanoscale*. 2017;9:16357–16364. doi:10.1039/C7NR05577C

51. Li X, Wei L, Pan L, et al. Homogeneous immunosorbent assay based on single-particle enumeration using upconversion nanoparticles for the sensitive detection of cancer biomarkers. *Anal Chem*. 2018;90:4807–4814. doi:10.1021/acs.analchem.8b00251

52. Farka Z, Mickert MJ, Hlaváček A, et al. Upconversion-linked immunosorbent assay with extended dynamic range for the sensitive detection of diagnostic biomarkers. *Anal Chem*. 2017;89:11825–11830. doi:10.1021/acs.analchem.7b03542

53. Wang P, Joshi P, Alazemi A, et al. Upconversion nanoparticle-based ligase-assisted method for specific and sensitive detection of T790M mutation in epidermal growth factor receptor. *Biosens Bioelectron*. 2014;62:120–126. doi:10.1016/j.bios.2014.06.037

54. Xu XZ, Zhang XY, Wu YL, et al. Folic acid-conjugated GdPO$_4$:tb^{3+}@SiO$_2$nanoprobe for folate receptor-targeted optical and magnetic resonance bi-modal imaging. *J Nanopart Res*. 2016;18:334. doi:10.1007/s11051-016-3649-x

55. Vaneckova T, Smerkova K, Zitka J, et al. Upconversion nanoparticle bioconjugates characterized by capillary electrophoresis. *Electrophoresis*. 2018;39:2246–2252. doi:10.1002/elps.201700483

56. Lan JM, Li L, Liu YX, et al. Upconversion luminescence assay for the detection of the vascular endothelial growth factor, a biomarker for breast cancer. *Microchim Acta*. 2016;183:3201–3208. doi:10.1007/s00604-016-1965-6

57. Cao T, Yang Y, Gao Y, et al. High-quality water-soluble and surface-functionalized upconversion nanocrystals as luminescent probes for bioimaging. *Biomaterials*. 2011;32:2959–2968. doi:10.1016/j.biomaterials.2010.12.050

58. Kumar R, Nyk M, Ohulchanskyy TY, et al. Combined optical and MR bioimaging using rare earth ion doped NaYF$_4$ nanocrystals. *Adv Funct Mater*. 2009;19:853–859. doi:10.1002/adfm.200800765

59. Han G, Li H, Huang X, et al. Simple synthesis of carboxyl-functionalized upconversion nanoparticles for biosensing and bioimaging applications. *Talanta*. 2016;147:207–212. doi:10.1016/j.talanta.2015.09.059

60. Hu H, Xiong L, Zhou J, et al. Multimodal-luminescence core-shell nanocomposites for targeted imaging of tumor cells. *Chem Eur J*. 2009;15:3577–3584.

61. Han G, Jiang H, Huo Y, et al. Simple synthesis of amino acid-functionalized hydrophilic upconversion nanoparticles capped with both carboxyl and amino groups for bimodal imaging. *J Mater Chem B*. 2016;4:3351–3357. doi:10.1039/C6TB00650G

62. Yu XF, Sun Z, Li M, et al. Neurotoxin-conjugated upconversion nanoprobes for direct visualization of tumors under near-infrared irradiation. *Biomaterials*. 2010;31:8724–8731. doi:10.1016/j.biomaterials.2010.07.099

63. Xiong L, Chen Z, Tian Q, et al. High contrast upconversion luminescence targeted imaging in vivo using peptide-labeled nanophosphors. *Anal Chem*. 2009;81:8687–8694. doi:10.1021/ac901960d

64. Sun L, Wei Z, Chen H, et al. Folic acid-functionalized up-conversion nanoparticles: toxicity studies in vivo and in vitro and targeted imaging applications. *Nanoscale*. 2014;6:8878. doi:10.1039/C4NR02312A

65. Song E, Zhang Z, Luo Q, et al. Tumor cell targeting using folate-conjugated fluorescent quantum dots and receptor-mediated endocytosis. *Clin Chem*. 2009;55:955–963. doi:10.1373/clinchem.2008.113423

66. Sega EI, Low PS. Tumor detection using folate receptor-targeted imaging agents. *Cancer Metastasis Rev*. 2008;27:655–664. doi:10.1007/s10555-008-9155-6

67. Chávez D, Juarez K, Campos CH, et al. Cytotoxicity, genotoxicity and uptake detection of folic acid-functionalized green upconversion nanoparticles Y$_2$O$_3$/Er^{3+}, Yb^{3+} as biolabels for cancer cells. *J Mater Sci*. 2018;53:6665–6680. doi:10.1007/s10853-017-1946-0

68. Dong S, Xu J, Jia T, et al. Upconversion-mediated ZnFe$_2$O$_4$ nanoplatform for NIR-enhanced chemodynamic and photodynamic therapy. *Chem Sci*. 2019;10:4259–4271. doi:10.1039/C9SC00387H

69. Dai ZF, editor. *Advances in Nanotheranostics. Springer Series in Biomaterials Science and Engineering*. Springer-Verlag. Vol. 6; 2016

70. Castano AP, Mroz P, Hamblin MR, et al. Photodynamic therapy and anti-tumour immunity. *Nat Rev Cancer*. 2006;6:535–545. doi:10.1038/nrc1894

71. Li Z, Zhang Y, La H, et al. Upconverting NIR photons for bioimaging. *Nanomaterials*. 2015;5:2148–2168. doi:10.3390/nano5042148

72. Idris NM, Jayakumar MKG, Bansal A, et al. Upconversion nanoparticles as versatile light nanotransducers for photoactivation applications. *Chem Soc Rev*. 2015;44:1449–1478. doi:10.1039/C4CS00158C

73. Punjabi A, Wu X, Tokatli A, et al. Amplifying the red-emission of upconverting nanoparticles for biocompatible clinically used prodrug-induced photodynamic therapy. *ACS Nano*. 2014;8:10621–10630. doi:10.1021/nn505051d

74. Liu C, Liu B, Zhao J, et al. Nd^{3+}-sensitized upconversion metal organic frameworks for mitochondria-targeted amplified photodynamic therapy. *Angew Chem Int Ed*. 2020;59:2634–2638. doi:10.1002/anie.201911508

75. Zhu X, Feng W, Chang J, et al. Temperature-feedback upconversion nanocomposite for accurate photothermal therapy at facile temperature. *Nat Commun*. 2016;7:10437.

76. Chen Q, Wang C, Cheng L, et al. Protein modified upconversion nanoparticles for imaging-guided combined photothermal and photodynamic therapy. *Biomaterials*. 2014;35:2915–2923. doi:10.1016/j.biomaterials.2013.12.046

77. Yu X, Lao Y, Teng X, et al. SENP3 maintains the stability and function of regulatory T cells via BACH2 deSUMOylation. *Nat Commun*. 2018;9:3157. doi:10.1038/s41467-018-05676-6

78. Wang H, Su X, Yang M, et al. Reciprocal control of miR-197 and IL-6/STAT3 pathway reveals miR-197 as potential therapeutic target for hepatocellular carcinoma. *Oncoimmunology*. 2015;4:1031440. doi:10.1080/2162402X.2015.1031440

79. Lv W, Yang T, Yu Q, et al. A phosphorescent Iridium(III) complex-modified nanoprobe for hypoxia bioimaging via time-resolved luminescence microscopy. *Adv Sci*. 2015;2:1500107. doi:10.1002/advs.201500107

80. Xing QJ, Li NJ, Jiao Y, et al. Near-infrared light-controlled drug release and cancer therapy with polymer-caged upconversion nanoparticles. *RSC Adv*. 2015;5:5269–5276. doi:10.1039/C4RA12678E

81. Yang CN, Liu QL, He DC, et al. Dual-modal imaging and photodynamic therapy using upconversion nanoparticles for tumor cells. *Analyst*. 2014;139:6414–6420.

82. Bi H, Dai Y, Yang P, et al. Glutathione mediated size-tunable UCNPs-Pt(IV)-$ZnFe_2O_4$ nanocomposite for multiple bioimaging guided synergetic therapy. *Small*. 2018;14:1703809. doi:10.1002/smll.201703809

83. Yuan Y, Xu L, Dai S, et al. A facile supramolecular approach to fabricate multifunctional upconversion nanoparticles as a versatile platform for drug loading in vivo delivery and tumor imaging. *J Mater Chem B*. 2017;5:2425–2435. doi:10.1039/C6TB03381D

84. Zeng T, Zhang T, Wei W, et al. Compact, programmable, and stable biofunctionalized upconversion nanoparticles prepared through peptide-mediated phase transfer for high-sensitive protease sensing and in vivo apoptosis imaging. *ACS Appl Mater Interfaces*. 2015;7:11849–11856. doi:10.1021/acsami.5b01446

85. Chen J, Zhang DY, Zou Y, et al. Developing a pH-sensitive $Al(OH)_3$ layer-mediated UCNP@$Al(OH)_3$/Au nanohybrid for photothermal therapy and fluorescence imaging in vivo. *J Mater Chem B*. 2018;6:7862–7870. doi:10.1039/C8TB02213E

86. Wang C, Chen L, Liu YM, et al. Imaging-guided pH-sensitive photodynamic therapy using charge reversible upconversion nanoparticles under near-infrared light. *Adv Funct Mater*. 2013;23:3077–3086.

87. Ding CP, Cheng SS, Zhang CL, et al. Ratiometric upconversion luminescence nanoprobe with near-infrared Ag_2S nanodots as the energy acceptor for sensing and imaging of pH in vivo. *Anal Chem*. 2019;91:7181–7188. doi:10.1021/acs.analchem.9b00404

88. Li H, Lei W, Wu J, et al. An upconverting nanotheranostic agent activated by hypoxia combined with NIR irradiation for selective hypoxia imaging and tumour therapy. *J Mater Chem B*. 2018;6:2747–2757. doi:10.1039/C8TB00637G

89. Niu N, Zhang Z, Gao X, et al. Photodynamic therapy in hypoxia: near-infrared-sensitive, self-supported, oxygen generation nano-platform enabled by upconverting nanoparticles. *Chem Eng J*. 2018;352:818–827. doi:10.1016/j.cej.2018.07.049

90. Xu J, Han W, Yang PP, et al. Tumor microenvironment-responsive mesoporous MnO_2-coated upconversion nanoplatform for self-enhanced tumor theranostics. *Adv Funct Mater*. 2018;28:1803804. doi:10.1002/adfm.201803804

91. Li F, Du Y, Liu J, et al. Responsive Assembly of upconversion nanoparticles for pH-activated and near-infrared-triggered photodynamic therapy of deep tumors. *Adv Mater*. 2018;30:e1802808. doi:10.1002/adma.201802808

92. Liu S, Li W, Gai S, et al. A smart tumor microenvironment responsive nanoplatform based on upconversion nanoparticles for efficient multimodal imaging guided therapy. *Biomater Sci*. 2019;7:951–962.

93. Shi J, Kantoff PW, Wooster R, et al. Cancer nanomedicine: progress, challenges and opportunities. *Nat Rev Cancer*. 2017;17:20–37.

94. Hou Z, Zhang Y, Deng K, et al. UV-emitting upconversion-based TiO_2 photosensitizing nanoplatform: near-infrared light mediated in vivo photodynamic therapy via mitochondria-involved apoptosis pathway. *Acs Nano*. 2015;9:2584–2599. doi:10.1021/nn506107c

95. Bazylińska U, Wawrzyńczyk D, Szewczyk A, et al. Engineering and biological assessment of double core nanoplatform for co-delivery of hybrid fluorophores to human melanoma. *J Inorg Biochem*. 2020;208:111088. doi:10.1016/j.jinorgbio.2020.111088

96. Wawrzyńczyk D, Cichy B, Zaręba JK, et al. On the interaction between up-converting $NaYF^4:Er^{3+}$, Yb^{3+} nanoparticles and Rose Bengal molecules constrained within the double core of multi-functional nanocarriers. *J Mater Chem C*. 2019;7:15021–15034. doi:10.1039/C9TC04163J

97. Buchner M, García Calavia P, Muhr V, et al. Photosensitiser functionalised luminescent upconverting nanoparticles for efficient photodynamic therapy of breast cancer cells. *Photochem Photobiol Sci*. 2019;18:98–109. doi:10.1039/C8PP00354H

98. Chen G, Roy I, Yang C, et al. Nanochemistry and nanomedicine for nanoparticle-based diagnostics and therapy. *Chem Rev*. 2016;116:2826–2885. doi:10.1021/acs.chemrev.5b00148

99. Li H, Wang X, Huang D, et al. Recent advances of lanthanide-doped upconversion nanoparticles for biological applications. *Nanotechnology*. 2020;31:072001. doi:10.1088/1361-6528/ab4f36

100. Abualrejal M, Kamel E, Rong T, et al. Rational synthesis of three-dimensional core-double shell upconversion nanodendrites with ultrabright luminescence for bioimaging application. *Chem Sci*. 2019;10:7591–7599. doi:10.1039/C9SC01586H

101. Lay A, Sheppard H, Siefe C, et al. Optically robust and biocompatible mechanosensitive upconverting nanoparticles. *ACS Cent Sci*. 2019;5:1211–1222. doi:10.1021/acscentsci.9b00300

102. Wang F, Zhang C, Qu X, et al. Cationic cyanine chromophore-assembled upconversion nanoparticles for sensing and imaging H_2S in living cells and zebrafish. *Biosens Bioelectron*. 2019;126:96–101. doi:10.1016/j.bios.2018.10.056

103. Wang H, Wang Z, Tu Y, et al. Homotypic targeting upconversion nano-reactor for cascade cancer starvation and deep-tissue phototherapy. *Biomaterials*. 2020;235:119765. doi:10.1016/j.biomaterials.2020.119765

104. Qu A, Wu X, Li S, et al. An NIR-responsive DNA-mediated nanotetrahedron enhances the clearance of senescent cells. *Adv Mater.* 2020;32:2000184. doi:10.1002/adma.202000184

105. Sun Y, Feng W, Yang P, et al. The biosafety of lanthanide upconversion nanomaterials. *Chem Soc Rev.* 2015;44:1509–1525. doi:10.1039/C4CS00175C

106. Cheng L, Yang K, Shao M, et al. In vivo pharmacokinetics, long-term biodistribution and toxicology study of functionalized upconversion nanoparticles in mice. *Nanomedicine.* 2011;6:1327–1340. doi:10.2217/nnm.11.56

107. Bazylińska U, Wawrzyńczyk D. Encapsulation of TOPO stabilized $NaYF_4$: er^{3+}, Yb^{3+} nanoparticles in biocompatible nanocarriers: synthesis, optical properties and colloidal stability. *Colloid Surface A.* 2017;532:556–563. doi:10.1016/j.colsurfa.2017.03.040

108. Chu H, Zhao J, Mi Y, et al. NIR-light-mediated spatially selective triggering of anti-tumor immunity via upconversion nanoparticle-based immunodevices. *Nat Commun.* 2019;10:2839. doi:10.1038/s41467-019-10847-0